Hindawi Publishing Corporation
Advances in Condensed Matter Physics
Volume 2013, Article ID 931726, 7 pages
http://dx.doi.org/10.1155/2013/931726

Research Article

Aging Effect on Electrical Conductivity of Pure and Al-Doped $YBa_2Cu_3O_{7-\delta}$ Single Crystals with a Given Topology of Planar Defects

Ruslan V. Vovk,[1] Nikolaj R. Vovk,[1] and Oleksandr V. Dobrovolskiy[1,2]

[1] *Physical Department, Kharkiv National University, Kharkiv 61077, Ukraine*
[2] *Physikalisches Institut, Goethe-University, 60438 Frankfurt am Main, Germany*

Correspondence should be addressed to Oleksandr V. Dobrovolskiy; dobrovolskiy@physik.uni-frankfurt.de

Received 18 August 2013; Accepted 25 September 2013

Academic Editor: Hechang Lei

The conducting properties in the basal *ab* plane of pure and Al-doped $YBa_2Cu_3O_{7-\delta}$ single crystals before and after long-time exposure in air atmosphere are investigated. It is shown that prolonged aging leads to an increase of the density of effective scattering centers for the normal carriers. The aluminum doping has been revealed to partially slowdown the degradation of the conducting properties in process of aging. The excess conductivity, $\Delta\sigma(T)$, has been found to obey exponential dependence in the broad temperature range $T_c < T < T^*$. In the pseudogap regime, the mean-field transition temperature T^* and the 3D-2D crossover point in the excess conductivity have been quantified. Near the critical temperature, $\Delta\sigma(T)$ is described well within the Aslamazov-Larkin theoretical model. Herewith, both aluminum doping and prolonged aging have been found to essentially expand the temperature interval of implementation of the pseudogap state, thus narrowing the linear section in the dependence $\rho_{ab}(T)$.

1. Introduction

Despite the fact that almost three decades have passed since the discovery of high-temperature superconductivity (HTSC) [1], the microscopic nature of this phenomenon remains definitively unexplained so far. In accordance with the contemporary views, it is assumed that the key for understanding the nature of HTSC can be in scrutinizing the physical phenomena observed in these compounds in the normal state at temperatures at and above the critical temperature T_c. The transitions to the fluctuation and the pseudogap regimes are exemplary for those phenomena. Whereas thousands of papers are devoted to the treatment of physics of the pseudogap state and the fluctuation conductivity in HTSC compounds (see, e.g., [2–6] for reviews), both the nature of the pseudogap state to appear and its role in the formation of the superconducting state still remain unclear.

Along with this, in the recent years there is a tendency to expand the field of studies regarding the technological use of high-temperature superconductors (HTSCs) [7]. This is mostly associated with a more intensive use of these compounds in contemporary microelectronics, telecommunication systems, and so forth. In this respect, compounds from the system $YBa_2Cu_3O_{7-\delta}$ (1-2-3) are most promising. This is due to several factors as follows. (i) These superconductors have a high critical temperature T_c, above the boiling point of liquid nitrogen. (ii) One can relatively easy alter their structure and conductive properties by varying the oxygen content [8] and by substituting the constituent elements with respective isoelectronic analogues [9]. It should be noted that, in 1-2-3 compounds, there practically always exist planar defects, such as twin boundaries (TBs) that can significantly extend the range of possible research [10]. At the same time, all the aforementioned characteristics are raising new questions and challenges. For example, the presence of labile oxygen in $YBa_2Cu_3O_{7-\delta}$ often leads to a nonequilibrium state in the system, which can be induced by temperature [8, 9] or by high pressure [10–12]. In general, these effects are observed in nonstoichiometric samples in respect of the oxygen content and are absent in samples with low oxygen

deficiency $\delta \leq 0.15$ [13]. At the same time, in the literature, there are a number of works [14–16] which note the possibility of changing the superconducting and electrotransport properties of 1-2-3 samples in the course of prolonged aging in air atmosphere. Therein, the published data are often contradictory. For instance, a significant improvement of the electrotransport and an increase of the critical current in process of long-term annealing are reported in [17]. At the same time, a pronounced degradation of these properties before long-term exposure in ambient air is noted in [14–16].

Altering the composition of 1-2-3 superconductors is also an important instrument to find empirical ways for improving their critical parameters and for extending their technological applications. It is known that a complete or partial substitution of yttrium with rare earth elements, with the exception of praseodymium (the praseodymium anomaly) which suppresses the superconducting parameters of the compound [18], slightly affects their physical characteristics in the normal and the superconducting state [9, 10, 19]. By contrast, an important role is played by the partial replacement of copper by elements such as gold, silver, and aluminum [20–24]. Gold and silver, in small concentrations of these compounds, improve conductivity and prevent degradation of the superconducting properties in the aging process [20, 21]. The published data regarding the impact of aluminum on the electrotransport properties of the compound $YBa_2Cu_3O_{7-\delta}$ still remain unclear and are in essence contradictory. For example, a slight rise in the resistivity ρ_{ab} in the basal *ab* plane of $YBa_2Cu_{3-y}Al_yO_{7-\delta}$ crystals at $y \leq 0.1$ was observed in [22]. At the same time, a twofold increase of ρ_{ab} at the same concentration of aluminum is reported in [23]. The reason for this discrepancy is most likely a nonhomogeneous distribution of aluminum over the crystal volume, as during the crystal growth in alundum crucibles the introduction of aluminum occurs in an uncontrolled way. In particular, the nonhomogeneous distribution of aluminum results in broader transitions into the superconducting state ($\Delta T_c \geq 2$ K) and their stepwise form [22, 23]. There is also substantial variation in the superconducting parameters of the samples. It should be noted that aluminum doping facilitates a severalfold reduction of the period of the twin superstructure [24] and, at high concentrations, the formation of intersecting "tweed"-type twin domains [25]. On the one hand, TBs, which are extended planar defects, promote strengthening of the pinning processes [26], thus extending the range of the use of HTSCs in obtaining high magnetic fields. On the other hand, the presence of TBs often complicates the investigation of the resistive characteristics, due to the difficulty of defining their contribution to the electrical conductivity in HTSCs [24]. Thereby, the influence of aluminum doping on aging of 1-2-3 compounds has remained an open question so far.

Taking the above under consideration, the objective of this study is to investigate, in the different conductivity regimes, the effect of prolonged aging in ambient air on the electrotransport properties of pure and Al-doped $YBa_2Cu_3O_{7-\delta}$ single crystals. The samples have a high critical temperature T_c and contain a system of unidirectional TBs. The measurements are carried out with the transport current **I** directed parallel to TBs, that is, when the influence of the TBs on the charge carrier scattering is minimal.

2. Sample Preparation

The $YBa_2Cu_3O_{7-\delta}$ single crystals were grown in a gold crucible by the solution-melting method, under small temperature gradient along the crucible [24]. As source components we used powder compounds of Y_2O_3, $BaCO_3$ and Cu. To obtain Al-doped single crystals, 0.2 at.% Al_2O_3 was added. After the growth, all the crystals were annealed at 420°C in air atmosphere in order to obtain the optimal oxygen concentration and a high T_c. In all the samples the axis **c** was oriented along the smallest dimension. For the resistivity measurements, the following single crystals were selected: crystal K1 ($YBa_2Cu_3O_{7-\delta}$) with dimensions of $2 \times 0.3 \times 0.02\,mm^3$ and crystal K2 ($YBa_2Cu_{3-y}Al_yO_{7-\delta}$) with dimensions of $2.3 \times 0.75 \times 0.03\,mm^3$. Both single crystals contained areas with unidirectional TBs, with dimensions of $0.5 \times 0.5\,mm^2$. The geometry was selected in such a way that we could cut out bridges with parallel TBs (see also Figure 1(a)), with a width of 0.2 mm and a distance between the voltage contacts of 0.3 mm. The standard four-contact scheme was used to form electric contacts, whose arrangement is shown in the inset of Figure 1(b). In these, gold connectors (0.05 mm in diameter) were attached to the sample surface with silver paste. To make the electrical contacts easier, both wired samples were thereupon annealed in ambient air for several hours. This method provided a contact transient resistance of less than 1 Ω and made it possible to measure the resistivity at transport currents up to 10 mA in the *ab* plane. The temperature was measured with a copper-constantan thermocouple. The first measurements of the electrical resistivity in the basal *ab* plane were made immediately after removal of the crystals from the melt and saturating them with oxygen to the optimum value ($\delta \leq 0.1$). After these measurements, the crystals were stored in a glass container until the remeasurements, which have been done 6 years later.

We performed an inspection of the elemental composition in the as-grown crystals using energy-dispersive X-ray spectroscopy (EDX). The EDX parameters were 10 kV/2.4 nA and the probed areas were $2 \times 2\,\mu m^2$. Here the beam energy determines the effective thickness of the layer being analyzed, which is approximately 0.7 μm. The penetration of the electrons into the crystal was calculated by the simulation program Casino available at http://www.gel.usherbrooke.ca/casino/index.html. The material composition was calculated taking into account ZAF (atomic number, absorption, and fluorescence) and background corrections. The software we used was EDAX's Genesis Spectrum v. 5.10. The statistical error in the elemental composition is 1%. The EDX spectrum for the pure crystal K1 is shown in Figure 1(b). It shows four peaks corresponding to 7.7 at.% of Y, 16.2 at.% of Ba, 23.1 at.% of Cu, and 53 at.% of O. Other elements have not been detected in the as-grown pure crystal K1.

A photograph of the surface of the Al-doped crystal K2, with a characteristic pattern of TBs, is shown in Figure 1(a). As is known, substitutions of 3-valent ions are centers for

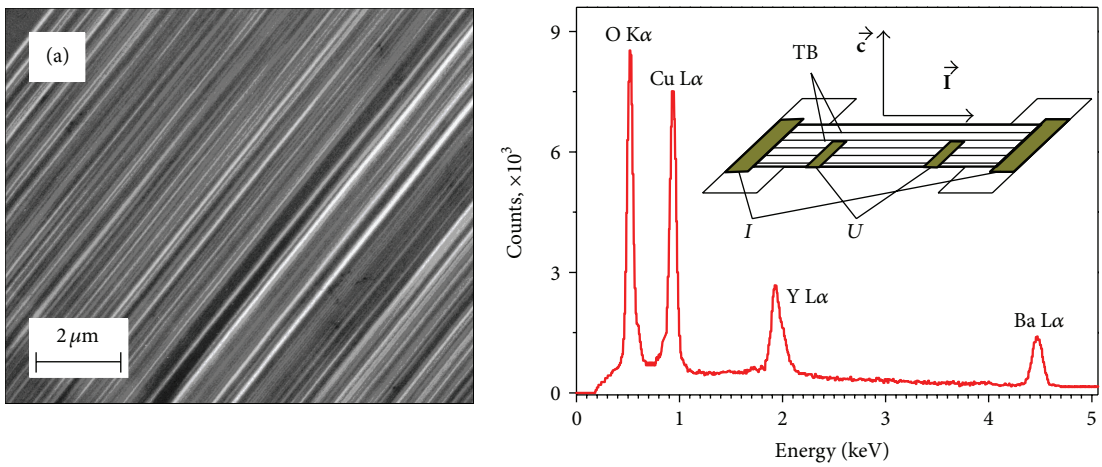

FIGURE 1: (a) Photograph of the section with unidirectional twin boundaries in the Al-doped crystal K2. (b) Main panel: Material composition in the as-grown pure crystal K1 revealed by energy-dispersive X-ray spectroscopy (probed area of $2 \times 2\,\mu m^2$). Inset: Geometry of the experiment, see text for details.

the defect formation [24, 25]. As their concentration increases, the period of the domain structure decreases. As a consequence of this, neighboring microtwins overlap and a tweed-like structure results [25]. As it is evident from Figure 1(a), such a tweed-like structure is absent in the investigated crystal of $YBa_2Cu_{3-y}Al_yO_{7-\delta}$. This must be attributed to the low concentration of Al. We also note that the twin-to-twin distance in the Al-doped crystal K2 is a factor of 2-3 smaller than that in the pure crystal K1.

3. Results and Discussion

The temperature dependences of the electrical resistivity in the *ab* plane $\rho_{ab}(T)$ of crystals K1 and K2, measured before and after prolonged aging in air atmosphere, are shown in Figures 2(a) and 2(b), respectively. The superconducting transitions for the same samples are shown in ρ_{ab}-T and $d\rho_{ab}/dT$-T coordinates in the respective insets. One can see that in all the cases the dependences are quasimetallic. However, the ratio $\rho_{ab}(300\,K)/\rho_{ab}(0\,K)$ measured for the as-grown and aged samples has diminished from 64 to 39 and from 12 to 8 for crystals K1 and K2, respectively. Here, the value of $\rho_{ab}(0\,K)$ was determined by extrapolating the linear section in $\rho_{ab}(T)$, as shown by the dashed lines in Figure 2. At the same time, the resistivity $\rho_{ab}(300\,K)$ of crystals K1 and K2 has risen from 151 to 196 and from 421 to 453 $\mu\Omega$cm, accordingly. This has been accompanied by the respective reduction of their critical temperature from 91.75 to 90.83 and from 92.05 to 90.85 K. In our measurements, the critical temperature T_c was determined as that corresponding to the maximum in the dependence $d\rho_{ab}(T)/dT$. For both aged samples, the width of the superconducting transition, ΔT_c, has noticeably increased (from 0.3 and 0.5 to $\approx$1 K for crystals K1 and K2, resp.), and the transition of crystal K2 has gained a stepwise shape. The measured and calculated parameters of the investigated samples are compiled in Table 1. Using the literature data for the dependence of T_c on the oxygen concentration [27], one can arrive at the conclusion that in both aged crystals its content has insufficiently (by 1-2%) decreased and is within $\delta \leq 0.15$ [27]. The broadening of the resistive transitions for both crystals reflects a decrease in homogeneity of the investigated samples [9, 10, 12, 13], whereas the stepwise shape of the transition in the remeasurements on crystal K2 testifies that the phase segregation appeared in its volume [10, 12]. The latter assumption is supported by the presence of a series of peaks in the dependence $d\rho_{ab}(T)/dT$ of crystal K2. According to [9], such peaks correspond to T_c of different phases in the crystal volume. The absence of peaks for crystal K1 suggests that percolation pathways are likely to ensue for the current flow through the phase with a higher T_c [28].

As it follows from Figure 2 and Table 1, the relative change in the resistive parameters during the aging process is more pronounced for the pure crystal K1 than for the Al-doped K2. As the current **I** is applied parallel to TBs in all the samples, this difference cannot be caused by the enhanced density of TBs in crystal K2 exhibiting a smaller twin-to-twin distance. The observed increase of ρ_{ab} for the aged samples must be caused by a decrease of the density of the charge carriers or the appearance of effective scattering centers. This is also supported by the reduction of the ratio $\rho_{ab}(300\,K)/\rho_{ab}(0\,K)$. The role of such scattering centers may be played by an increasing number of vacancies that appeared in the aged samples and by a rise in nonstoichiometry of the compound, most likely owing to losses of oxygen. Along with increasing ρ_{ab}, as already mentioned above, a series of peaks have appeared in $d\rho_{ab}/dT$ of sample K2. This must assert the risen number of different phase inclusions [28] in the crystal volume. As is known [24], impurities of the 3-valent Al have a significantly smaller radius than the one that Cu has, thereby providing the centers for the defects formation. In these, aluminum atoms can form a specific octahedral environment of oxygen atoms [24] that, in turn, can facilitate the segregation of the conducting subsystem into several phases with different T_c. The presence of such

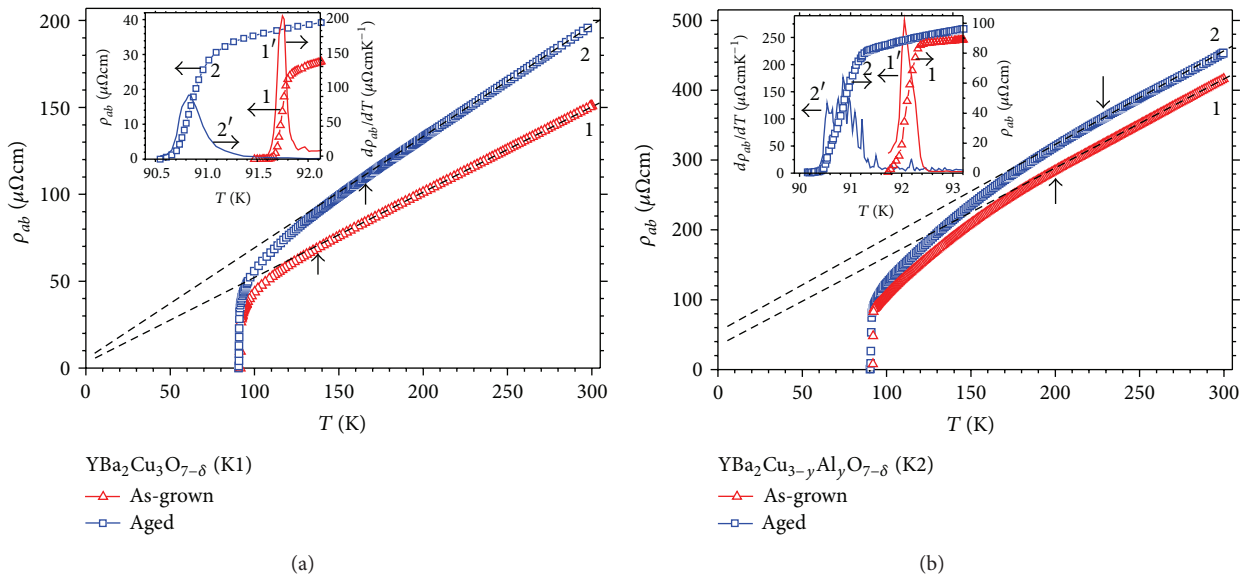

FIGURE 2: The temperature dependence $\rho_{ab}(T)$ of the single crystals (a) $YBa_2Cu_3O_{7-\delta}$ and (b) $YBa_2Cu_{3-y}Al_yO_{7-\delta}$ before and after long aging in ambient air, curves 1 and 2, respectively. The arrows show the mean-field transition temperature T^* to the pseudogap regime. The extrapolated values of $\rho_{ab}(0\,\mathrm{K})$ are traced by the dashed straight lines. The insets show the superconducting transitions in ρ_{ab}-T and $d\rho_{ab}/dT$-T coordinates for the same samples. The numbering of the curves in the insets corresponds to that in the main panels.

TABLE 1: Resistivity parameters of the as-grown and aged samples.

No	Sample	T_c, K	ρ_{ab} (300 K), $\mu\Omega$cm	T^*, K	Δ^*_{ab}, meV	$\tan\alpha_{3D}$	$\tan\alpha_{2D}$	ε_0	$\xi_c(0)$, Å
K1	as-grown	91.75	151	138	88.7	−0.508	−1.084	0.061	1.45
	aged	90.83	196	167	66.3	−0.503	−1.062	0.088	1.74
K2	as-grown	92.05	421	199	58.1	−0.506	−0.990	0.157	2.32
	aged	90.85	453	228	45.5	−0.495	−1.017	0.188	2.54

phases can become apparent via a stepwise shape of the superconducting transition (and the respective peaks in $d\rho_{ab}/dT$-T coordinates) [9, 10, 12, 13], as well as a change in the mechanism of diffusion processes and, thus, a reduction of the intensity of deoxygening of the sample volume.

As it is seen in Figure 2, with a decrease of the temperature below the characteristic value T^*, the dependence $\rho_{ab}(T)$ starts to deviate from the straight line. This fact proves the appearance of some excess conductivity which, according to the contemporary views, is stipulated by the transition into the pseudogap state (PG) [29–31]. At present, two main scenarios for the PG anomaly to appear in HTSC systems are discussed in the literature. In accordance with the first one, the appearance of the PG is connected with the short-range fluctuations of the "dielectric" type occurring in underdoped compounds [29]. Another scenario assumes the formation of Cooper pairs already at temperatures substantially higher than the critical temperature $T^* \gg T_c$, where T^* is the onset temperature of the PG state. This is followed by the establishment of the phase coherence at $T < T_c$ [30, 31]. As it is seen from Table 1 and Figure 2, prolonged aging leads to a pronounced narrowing of the linear section in $\rho_{ab}(T)$ for both crystals as compared to the respective as-grown samples. Along with this, the temperature T^* shifts towards higher temperatures by 29 K for both crystals K1 and K2. This results in an expansion of the temperature range for the excess conductivity to become apparent.

We turn now to a quantitative analysis of the observed changes in the excess conductivity. The temperature dependence $\Delta\sigma(T)$ is defined by the following relation:

$$\Delta\sigma(T) = \sigma(T) - \sigma_0, \tag{1}$$

where $\sigma_0 = \rho_0^{-1}$ is the conductivity determined by extrapolating the linear section down to the zero-temperature value, and $\sigma(T) = \rho^{-1}(T) = (A + BT)^{-1}$ is the experimentally measured conductivity value in the normal state. The thus calculated dependences $\Delta\sigma(T)$ are presented in $\ln\Delta\sigma$-$1/T$ coordinates in the main panels of Figures 3(a) and 3(b). It is seen in Figure 3 that the curves $\Delta\sigma(T)$ demonstrate linear behavior in a quite broad temperature range. This corresponds to their description by an exponential dependence of the following form:

$$\Delta\sigma(T) \propto \exp\left(\frac{\Delta^*_{ab}}{T}\right), \tag{2}$$

where Δ^*_{ab} determines some thermally activated process over the energy gap called "pseudogap". An exponential dependence $\Delta\sigma(T)$ was previously observed in YBaCuO

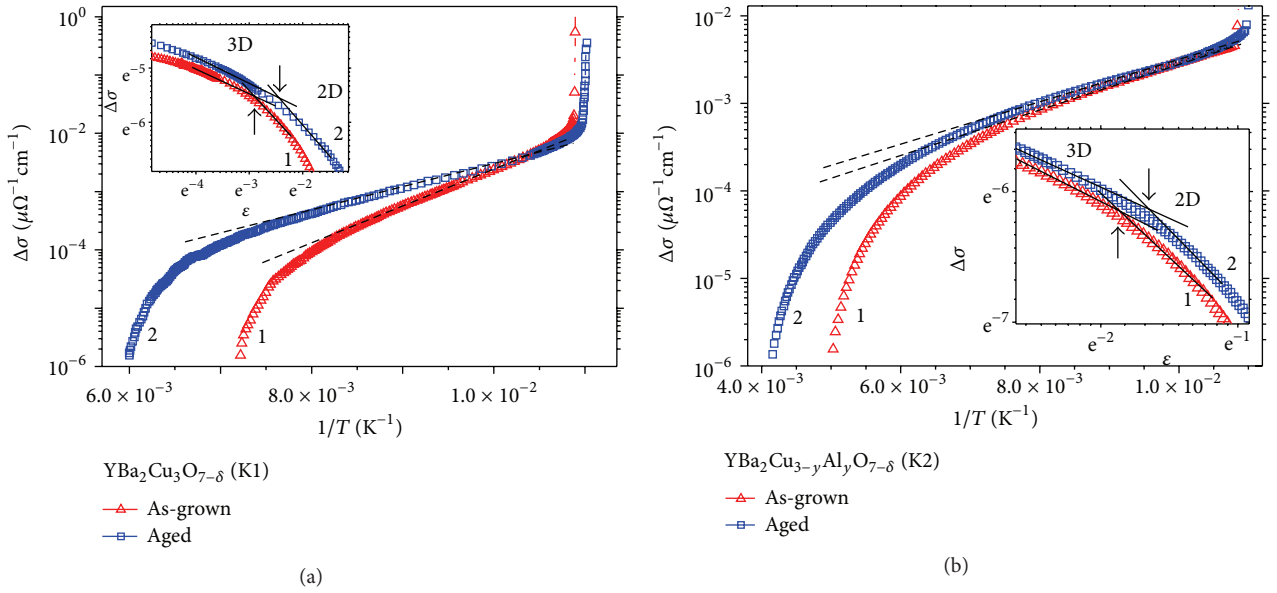

FIGURE 3: The temperature dependence of the excess conductivity $\Delta\sigma(T)$ in the *ab* plane of the single crystals (a) $YBa_2Cu_3O_{7-\delta}$ and (b) $YBa_2Cu_{3-y}Al_yO_{7-\delta}$ before and after long aging in air, in $\ln\Delta\sigma$-$1/T$ (main panels) and $\ln\Delta\sigma$-$\ln\varepsilon$ coordinates (insets). The dashed straight lines are fits by (2). In the insets, the solid straight lines are linear fits with slopes $\tan\alpha_{3D} \approx -0.5$ (3D regime) and $\tan\alpha_{2D} \approx -1$ (2D regime). The arrows show the 3D-2D crossover point. The numbering of the curves is the same as in Figure 2.

samples [13]. The fitting range of the experimental data can be substantially extended by introducing the factor $(1 - T/T^*)$. In this case, the excess conductivity turns out to be proportional to the density of superconducting carriers, $n_s \propto (1 - T/T^*)$, and inversly proportional to the number of pairs $\propto \exp(-\Delta^*_{ab}/kT)$ destroyed by thermal motion. Here T^* is regarded as the mean-field transition temperature to the PG regime, and the temperature range $T_c < T < T^*$, where the PG state exists, is determined by the rigidity of the order parameter phase. The latter, in turn, depends on the oxygen deficiency and the concentration of the doping element. Other specific mechanisms of the quasiparticle interaction, such as those caused by structural or kinematic anisotropy of the system, can also be relevant [32, 33]. The values of Δ^*_{ab} calculated by (2) for our samples are presented in Table 1. It is evident that the prolonged aging leads to the substantial suppression of the absolute value of the PG; namely, $\Delta^*_{ab1}/\Delta^*_{ab2} = 1.34$ and $\Delta^*_{ab1}/\Delta^*_{ab2} = 1.28$ for crystals K1 and K2, respectively.

As it follows from the main panels of Figure 3, with approaching T_c, a sharp rise in $\Delta\sigma(T)$ ensues. From the Aslamazov-Larkin theory [34], it is known that in the vicinity of T_c the excess conductivity is stipulated by the processes of fluctuational pairing of the charge carriers. The excess conductivity at $T > T_c$ for the two- (2D) and three-dimensional (3D) cases is determined by the following power-law dependences:

$$\Delta\sigma_{2D} = \frac{e^2}{16\hbar d}\varepsilon^{-1}, \tag{3}$$

$$\Delta\sigma_{3D} = \frac{e^2}{32\hbar\xi_c(0)}\varepsilon^{-1/2}, \tag{4}$$

where $\varepsilon = (T - T_c)/T_c$ is the reduced temperature, e is the electron charge, $\xi_c(0)$ is the coherence length along the axis **c** at $T \to 0$, and d is the characteristic dimension of the 2D layer.

To deduce the exponents determining the prevailing regime, the temperature dependences $\Delta\sigma(T)$ are plotted in $\ln\Delta\sigma$-$\ln\varepsilon$ coordinates in the insets of Figure 3. From these plots, it is seen that, in the vicinity of T_c, both dependences can be fitted well by straight lines with a tilt angle $\tan\alpha_{3D} \approx -0.5$ corresponding to the exponent $-1/2$ in (4). This evidently asserts the 3D character of the fluctuational superconductivity in this temperature range. With a further increase of the temperature, the decrease of $\Delta\sigma$ speeds up essentially ($\tan\alpha_{2D} \approx -1$). This, in turn, can be treated as an indication of the dimensionality change in the fluctuation conductivity. As it follows from (3) and (4), in the 3D-2D crossover point,

$$\xi_c(0)\,\varepsilon_0^{-1/2} = \frac{d}{2}. \tag{5}$$

In this case, having deduced the value of ε_0 and using the literature data on the dependence of the lattice parameter on δ [35] ($d = 11.7$ Å), one can calculate $\xi_c(0)$. Such calculations show that after prolonged exposure the coherence length $\xi_c(0)$ has increased from 1.49 to 1.74 and from 2.32 to 2.54 Å for crystals K1 and K2, respectively. This is accompanied by a shift of the 3D-2D crossover temperature, $T_{3D\text{-}2D}$, towards higher temperatures; see also Table 1 and Figure 3.

As a generalization of the obtained results, the observed changes in the three determinative temperatures are presented in the form of a chart in Figure 4. This sketch allows one to grasp the impact of aluminum doping and prolonged aging on the implementation of the different conductivity

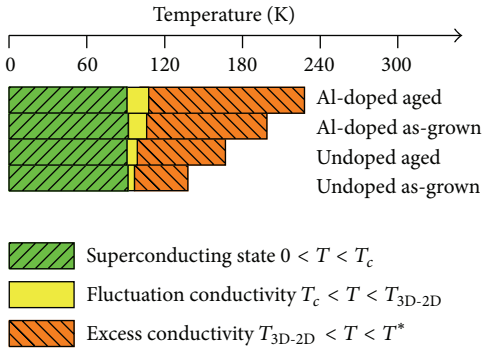

FIGURE 4: The impact of aluminum doping and prolonged aging on the implementation of the different conductivity regimes for the investigated single crystals of YBaCuO.

regimes in the investigated samples, in the entire temperature range. The three characteristic temperatures are the superconducting transition temperature T_c, the mean-field transition temperature to the pseudogap regime T^*, and the crossover temperature $T_{3D\text{-}2D}$ for the dimensionality change in the power-law dependence of the excess conductivity. We leave more subtle subregions, such as those corresponding to the critical fluctuations and noninteger dimensionality, as they are beyond the scope of this work. From Figure 4 it follows that both the 6-year aging and aluminum doping in the investigated concentration suppress T_c very slightly (by less than 1%). At the same time, when combining both of these treatments, the temperature range for the PG state to ensue is essentially expanded (by a factor of 2-3) towards higher temperatures. The increase of T^* due to aluminum doping is accompanied by a worth noting rise in $T_{3D\text{-}2D}$ (by about 10%), whereas $T_{3D\text{-}2D}$ remains almost unchanged in process of aging for both investigated samples.

4. Conclusion

In conclusion, let us sum up the main results obtained in this work. A long exposure of the optimally doped single crystals of YBaCuO in air atmosphere has been found to lead to an incomplete degradation of their conductive properties and to the appearance of effective scattering centers for the charge carriers. The introduction of Al impurities assists a partial slowdown of the degradation of the conducting properties in process of aging of the samples. The excess conductivity $\Delta\sigma(T)$ of the pure and Al-doped single crystals of YBaCuO obeys the exponential dependence in the broad temperature range $T_c < T < T^*$ and, in the case of approaching T_c, can be described well within the Aslamazov-Larkin theoretical model. The prolonged exposure of the samples leads to an essential broadening of the temperature range for the pseudogap state in the *ab* plane to ensue, thus narrowing the linear section in the dependence $\rho_{ab}(T)$. Along with this, indications of the phase segregation in the volume of the Al-doped sample have been observed. These become apparent via the presence of additional peaks in $d\rho_{ab}(T)/dT$ at temperatures close to the superconducting transition temperature.

Conflict of Interests

The authors declare that there is no conflict of interests.

Acknowledgments

Oleksandr V. Dobrovolskiy thanks Michael Huth for providing access to the scanning electron microscope and Evgeniya Begun for her help with EDX measurements. This work was supported in part by the European Commission within the Seventh Framework Programme (FP7), Project no. 247556. Oleksandr V. Dobrovolskiy acknowledges the Deutsche Forschungsgemeinschaft for financial support through Grant no. DO 1511/2-1.

References

[1] J. Bednorz and K. Müller, "Possible high-T_c superconductivity in the Ba-La- Cu-O system," *Zeitschrift für Physik B*, vol. 64, pp. 189–193, 1986.

[2] T. Timusk and B. Statt, "The pseudogap in high-temperature superconductors: an experimental survey," *Reports on Progress in Physics*, vol. 62, no. 1, pp. 61–122, 1999.

[3] T. Tohyama and S. Maekawa, "Angle-resolved photoemission in high T_c cuprates from theoretical viewpoints," *Superconductor Science and Technology*, vol. 13, no. 4, pp. R17–R32, 2000.

[4] M. L. Kulić, "Interplay of electron-phonon interaction and strong correlations: the possible way to high-temperature superconductivity," *Physics Reports*, vol. 338, no. 1-2, pp. 1–264, 2000.

[5] J. L. Tallon and J. W. Loram, "Doping dependence of T^*—what is the real high-T_c phase diagram?" *Physica C*, vol. 349, no. 1-2, pp. 53–68, 2001.

[6] H. G. Luo, Y. H. Su, and T. Xiang, "Scaling analysis of normal-state propertiesof high-temperature superconductors," *Physical Review B*, vol. 77, Article ID 014529, 2008.

[7] C. V. Varanasi, J. Burke, H. Wang, J. H. Lee, and P. N. Barnes, "Thick $YBa_2Cu_3O_{7-x}$ + $BaSnO_3$ films with enhanced critical current density at high magnetic fields," *Applied Physics Letters*, vol. 93, no. 9, Article ID 092501, 2008.

[8] J. D. Jorgensen, S. Pei, P. Lightfoor, H. Shi, A. P. Paulikas, and B. W. Veal, "Time-dependent structural phenomena at room temperature in quenched $YBa_2Cu_3O_{6.41}$. Local oxygen ordering and superconductivity," *Physica C*, vol. 167, no. 5-6, pp. 571–578, 1990.

[9] R. V. Vovk, M. A. Obolenskii, A. A. Zavgorodniy, I. L. Goulatis, V. I. Beletskii, and A. Chroneos, "Structural relaxation, metal-to-insulator transition and pseudo-gap in oxygen deficient $HoBa_2Cu_3O_{7-\delta}$ single crystals," *Physica C*, vol. 469, pp. 203–206, 2009.

[10] R. V. Vovk, Z. F. Nazyrov, M. A. Obolenskii, I. L. Goulatis, A. Chroneos, and V. M. Pinto Simoes, "Phase separation in oxygen deficient $HoBa_2Cu_3O_{7-\delta}$ single crystals: effect of high pressure and twin boundaries," *Philosophical Magazine*, vol. 91, no. 17, pp. 2291–2302, 2011.

[11] S. Sadewasser, J. S. Schilling, A. P. Paulikas, and B. W. Veal, "Pressure dependence of T_c to 17 GPa with and without relaxation effects in superconducting $YBa_2Cu_3O_x$," *Physical Review B*, vol. 61, no. 1, pp. 741–749, 2000.

[12] R. V. Vovk, G. Y. Khadzhai, Z. F. Nazyrov, I. L. Goulatis, and A. Chroneos, "Relaxation of the normal electrical

resistivity induced by high-pressure in strongly underdoped $YBa_2Cu_3O_{7-\delta}$ single crystals," *Physica B*, vol. 407, pp. 4470–4472, 2012.

[13] R. V. Vovk, N. R. Vovk, G. Y. Khadzhai, I. L. Goulatis, and A. Chroneos, "Effect of high pressure on the electrical resistivity of optimally doped $YBa_2Cu_3O_{7-\delta}$ single crystals with unidirectional planar defects," *Physica B*, vol. 422, pp. 33–35, 2013.

[14] Z. Li, H. Wang, N. Yang, X. Jin, and L. Shen, "Influence of air components on the stability of $YBa_2Cu_3O_{7-\delta}$," *Journal of the Chinese Ceramic Society*, vol. 18, no. 6, pp. 555–560, 1990.

[15] B. Martínez, F. Sandiumenge, S. Piñol, N. Vilalta, J. Fontcuberta, and X. Obradors, "Aging of critical currents and irreversibility line in melt textured $YBa_2Cu_3O_{7-\delta}$," *Applied Physics Letters*, p. 772, 1995.

[16] K. Schlesier, H. Huhtinen, S. Granroth, and P. Paturi, "An aging effect and its origin in GdBCO thin films," *Journal of Physics*, vol. 234, no. 1, Article ID 012036, 2010.

[17] Q.-R. Feng, X. Zhu, S.-Q. Feng, H. Zhang, and Z.-Z. Gan, "Effect of time aging on the properties of Ag-doped YBaCuO superconductors," *Superconductor Science and Technology*, vol. 6, no. 10, pp. 715–720, 1993.

[18] R. V. Vovk, Z. F. Nazyrov, I. L. Goulatis, and A. Chroneos, "Metal-to-insulator transition in $Y_{1-x}Pr_xBa_2Cu_3O_{7-\delta}$ single crystals with various praseodymium contents," *Physica C*, vol. 485, pp. 89–91, 2013.

[19] R. V. Vovk, M. A. Obolenskii, A. V. Bondarenko et al., "Transport anisotropy and pseudo-gap state in oxygen deficient $ReBa_2Cu_3O_{7-\delta}$ (Re = Y, Ho) single crystals," *Journal of Alloys and Compounds*, vol. 464, no. 1-2, pp. 58–66, 2008.

[20] M. Z. Cieplak, G. Xiao, C. L. Chien et al., "Incorporation of gold into $YBa_2Cu_3O_7$: structure and T_c enhancement," *Physical Review B*, vol. 42, no. 10, pp. 6200–6208, 1990.

[21] D. A. Lotnyk, R. V. Vovk, M. A. Obolenskii et al., "Evolution of the Fishtail-effect in pure and Ag-doped MG-YBCO," *Journal of Low Temperature Physics*, vol. 161, no. 3-4, pp. 387–394, 2010.

[22] R. B. Van Dover, L. F. Schneemeyer, J. V. Waszczak, D. A. Rudman, J. Y. Juang, and J. A. Cutro, "Extraordinary effect of aluminum substitution on the upper critical field of $YBa_2Cu_3O_7$: structure and T_c," *Physical Review B*, vol. 39, no. 4, pp. 2932–2935, 1989.

[23] B. Oh, K. Char, A. D. Kent et al., "Upper critical field, fluctuation conductivity, and dimensionality of $YBa_2Cu_3O_{7-x}$," *Physical Review B*, vol. 37, no. 13, pp. 7861–7864, 1988.

[24] R. V. Vovk, M. A. Obolenskii, Z. F. Nazyrov, I. L. Goulatis, A. Chroneos, and V. M. Pinto Simoes, "Electro-transport and structure of 1-2-3 HTSC single crystals with different plane defects topologies," *Journal of Materials Science*, vol. 23, pp. 1255–1259, 2012.

[25] G. Lacayo, G. Kästner, and R. Herrmann, "Twin to tweed transition in $YBa_2Cu_3O_{7-\delta}$ by substitution of Al for Cu," *Physica C*, vol. 192, no. 1-2, pp. 207–214, 1992.

[26] A. V. Bondarenko, V. A. Shklovskij, M. A. Obolenskii et al., "Resistivity investigations of plastic vortex creep in $YBa_2Cu_3O_{6.95}$ crystals," *Physical Review B*, vol. 58, no. 5, pp. 2445–2447, 1998.

[27] P. Schleger, W. Hardy, and B. Yang, "Thermodynamics of oxygen in $YBa_2Cu_3O_x$ between 450°C and 650°C," *Physica C*, vol. 176, pp. 261–273, 1991.

[28] R. V. Vovk, M. A. Obolenskii, A. A. Zavgorodniy et al., "Effect of high pressure on the fluctuation conductivity and the charge transfer of $YBa_2Cu_3O_{7-\delta}$ single crystals," *Journal of Alloys and Compounds*, vol. 453, no. 1-2, pp. 69–74, 2008.

[29] M. V. Sadovskii, I. A. Nekrasov, E. Z. Kuchinskii, T. Pruschke, and V. I. Anisimov, "Pseudogaps in strongly correlated metals: a generalized dynamical mean-field theory approach," *Physical Review B*, vol. 72, no. 15, Article ID 155105, 2005.

[30] R. V. Vovk, M. A. Obolenskii, A. A. Zavgorodniy, D. A. Lotnyk, and K. A. Kotvitskaya, "Temperature dependence of the pseudogap in aluminum and praseodymium-doped $YBa_2Cu_3O_{7-\delta}$ single crystals," *Physica B*, vol. 404, no. 20, pp. 3516–3518, 2009.

[31] E. Babaev and H. Kleinert, "Nonperturbative XY-model approach to strong coupling superconductivity in two and three dimensions," *Physical Review B*, vol. 59, no. 18, pp. 12083–12089, 1999.

[32] V. M. Apalkov and M. E. Portnoi, "Two-phonon scattering of magnetorotons in fractional quantum Hall liquids," *Physical Review B*, vol. 66, no. 12, Article ID 121303, 2002.

[33] P. J. Curran, V. V. Khotkevych, S. J. Bending, A. S. Gibbs, S. L. Lee, and A. P. MacKenzie, "Vortex imaging and vortex lattice transitions in superconducting Sr_2RuO_4 single crystals," *Physical Review B*, vol. 84, no. 10, Article ID 104507, 2011.

[34] L. G. Aslamasov and A. I. Larkin, "The influence of fluctuation pairing of electrons on the conductivity of normal metal," *Physics Letters A*, vol. 26, no. 6, pp. 238–239, 1968.

[35] G. D. Chryssikos, E. I. Kamitsos, J. A. Kapoutsis et al., "X-ray diffraction and infrared investigation of $RBa_2Cu_3O_7$ and $R_{0.5}Pr_{0.5}Ba_2Cu_3O_7$ compounds (RY and lanthanides)," *Physica C*, vol. 254, no. 1-2, pp. 44–62, 1995.